RESEARCH ARTICLE

INTERNATIONAL RESEARCH JOURNAL OF MULTIDISCIPLINARY TECHNOVATION

Asian Research Association

DOI: 10.54392/irjmt26215

Development of PPy/SWCNTs nanocomposite wrapped with Paraffin wax for EMI applications

O.V.P.R. Sivakumar [a], Arunmetha Sundaramoorthy [b,*], Dhineshbabu Nattanmai Raman [c], A. Geetha Rani [a]

[a] Department of Electronics and Communication Engineering, Geethanjali College of Engineering and Technology, Cheeryal(V), Keesara(M), Medchal- 501301, Telangana, India.

[b] Department of Electronics and Communication Engineering, KLEF Deemed to be University, Green Fields, Vaddeswaram - 522302, Andhra Pradesh, India.

[c] Department of Electronics and Communication Engineering, T. John Institute of Technology, Bengaluru – 560083, Karnataka, India

* Corresponding Author Email: sarunmetha@gmail.com

DOI: https://doi.org/10.54392/irjmt26215

Received: 04-12-2025; Revised: 02-03-2026; Accepted: 10-03-2026; Published: 28-03-2026

Abstract: In the process of developing stable, lightweight, cost-effective single-walled carbon nanotubes (SWCNTs; 1 wt% & 2.5 wt%)/Polypyrrole (PPy) nanocomposite films with paraffin wax, the films were prepared to address EMI problems in high-frequency radiation (radio/microwave), which are useful in day-to-day applications. The nanocomposite materials were prepared by the Solution mixing method, and the films were prepared using commercial Paraffin wax, with a thickness of about 1 mm. The nanocomposite materials were characterized using structural, behavioral, and morphological analyses. The Electrical conductivity of the composite films was further analyzed and found to increase significantly from 4.3 S m^{-1} (SP1W) to 11.8 S m^{-1} (SP2W), indicating enhanced percolation pathways with increased nanotube content. EMI Shielding Effectiveness (SE) was calculated using a unique approach that employed a microwave test bench and demonstrated total shielding effectiveness (SE) values of 6.02 dB and 7.73 dB for SP1W and SP2W, respectively, based on Voltage Standing Wave Ratio (VSWR) measurements. The improvement in SE is attributed to reduced skin depth (from 2.558 mm to 1.544 mm) and enhanced absorption loss (from 3.395 dB to 5.624 dB) at higher conductivity. Moreover, return loss (RL), Mismatch Loss (ML), Reflection Coefficient (RC), absorption loss, reflection loss, multiple reflections, and Shielding Effectiveness (SE) are also calculated from the VSWR. The result indicated that a higher weight percentage (2.5 wt%) of SWCNT yielded higher SE. The discussed results showed that the prepared PPy and SWCNT-based nanocomposite materials are suitable for EMI shielding applications.

Keywords: SWCNTs/PPy, Paraffin Wax, Microwave Test Bench, EMI Shielding

1. Introduction

Recent developments show that polymers are no longer limited to passive applications; they are evolving into active materials with conductive, electromagnetic, and optical properties [1]. EMI is an undesired effect of the proliferation of electronic systems in our current era of technological advancement. It is expected to disrupt or degrade the functionality of electronic devices, such as computers, medical equipment, Wi-Fi, and Bluetooth devices. To reduce electromagnetic radiation interference (radio waves and microwaves) with electronic devices, composite material approaches are employed. Generally, polymers alone are poor for EMI shielding [2-5]. However, by combining them with fillers such as carbon-based materials (CNTs, graphene, carbon fiber), metal nanoparticles, and magnetic ceramics, the conductivity and, therefore, the shielding effectiveness are significantly improved.

Conductive polymers like polyaniline, polypyrrole (PPy), polyacetylene, and polyindole contribute to EMI shielding without metallic fillers because they possess electrical conductivity. However, they have weaker mechanical properties compared to traditional polymers such as polyethylene, cellulose, polystyrene, and polyester. Poly(pyrrole) (PPy) is mechanically brittle, poorly soluble, and thus difficult to process on a large scale, making it unsuitable for practical applications. To address these challenges, various PPy composites have been synthesized and studied for their mechanical, electrical, and electronic properties [6-11].

Despite their impressive EMI shielding effectiveness, these binary PPy/CNT systems cannot reliably provide passive thermal management through latent heat storage, making them unsuitable for practical electronic device protection [12, 13]. Although paraffin wax/CNT sponge composites address both thermal management and EMI shielding, the absence of a conducting polymer component limits their shielding mechanism to conductive reflection, which can cause secondary electromagnetic pollution [14].

Although PPy/CNT composites have been widely studied for EMI shielding, they generally lack passive thermal buffering, which limits their ability to dissipate waste heat generated during extended electronic operation. Conversely, binary paraffin wax/CNT sponge (PW@CNS) composites exhibit both EMI shielding and thermal management through latent heat absorption. However, their shielding mechanism is mainly reflective due to the lack of strong dielectric polarization. PPy-coated CNT aerogel with paraffin wax was reported [15] solely for solar and electro-thermal energy conversion, without any characterization of EMI shielding. Additionally, PI/PPy-CNTs@PEG composites [16] incorporate a Phase Change Material (PCM). Still, they require high-temperature carbonization (700°C), use polyethylene glycol instead of paraffin wax, and focus on electromagnetic-wave absorption rather than EMI shielding.

Therefore, the present work is the first systematic investigation of a PPy/CNT/paraffin wax ternary composite specifically designed and tested for EMI shielding effectiveness, with the PPy enhancing inter-CNT. In contrast, paraffin wax offers passive, latent-heat-based thermal regulation—a unique combination that has not been previously reported. The first ternary PPy/CNT/paraffin wax composite was intentionally designed and evaluated for simultaneous absorption-dominant EMI shielding.

Considering these studies, PPy/SWCNTs nanocomposites were prepared using probe sonication. The samples serve as conductive fillers in a polymer matrix, and commercial paraffin wax was used to create hybrid nanocomposite films. The electromagnetic properties of the fabricated films were analyzed in the X-band frequency range with a specialized microwave test benchsetup. Paraffin wax was chosen as a polymer matrix in this study because of its low cost, chemical stability, lightweight nature, excellent barrier properties, phase-change behavior, and good thermal insulation properties [17]. Based on these attributes, paraffin wax was selected for use in this study.

2. Materials and Methods

Single-walled CNTs (SWCNTs) with a 1-2 nm diameter, 3-8 micrometers in length, and >98% purity were purchased from M/s Nanoshel. Polypyrrole (PPy) with a conductivity of 10-50 S/cm was purchased from M/s Sigma-Aldrich. Whatman Filter Paper (90 mm), acetone, and commercially available paraffin wax were purchased from M/s Sheth Chemicals.

2.1 Preparation of PPy/SWCNT nanocomposites

Solution mixing (as shown in Figure 1) was used to prepare single-walled carbon nanotube (SWCNT)-polypyrrole (PPy) nanocomposites. First, a magnetic stirrer bar was placed in a beaker containing 95 wt% PPy, and 20 mL of acetone was slowly added to the PPy solution. The mixture was stirred with a magnetic stirrer for 2 hours to ensure complete dissolution.

To improve the dispersion of SWCNTs in the PPy matrix and strengthen interfacial bonding, the SWCNTs were functionalized using a mixture of concentrated nitric acid (HNO_3) and sulfuric acid (H_2SO_4) in a 1:3 ratio. This mixture was subjected to ultrasonic irradiation at 20 kHz for 1 hour, with 5-minute intervals. The SWCNTs were then thoroughly washed with deionized water until the pH reached 7, dried in a vacuum oven at 60°C for 12 hours, and subsequently used in the nanocomposite for further analysis. As a result of this treatment, the surface of the SWCNTs was modified with carboxyl (-COOH) functional groups. The functionalized SWCNTs are referred to as FS.

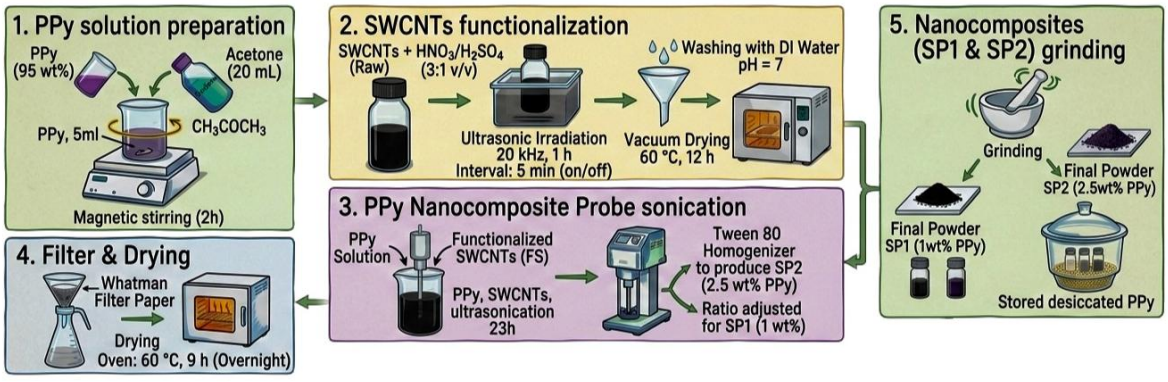

Figure 1. Methodology for Preparation of PPy/SWCNT nanocomposites

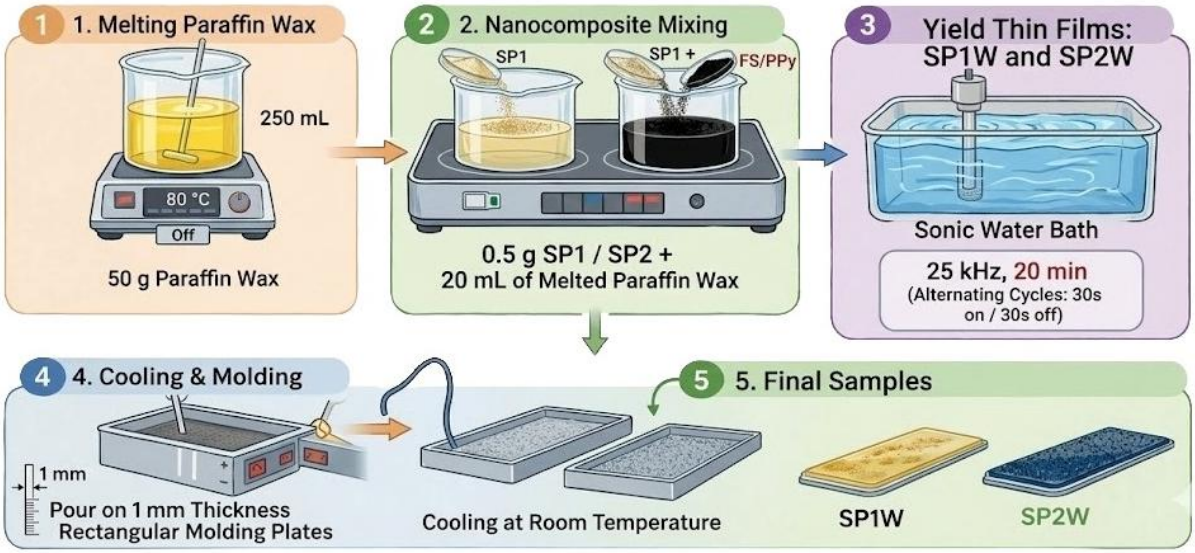

Figure 2. Methodology for Composite Film Preparation

After functionalization, 1 wt% and 2.5 wt% of FS were separately prepared and then added to the PPy solution. The mixture was further irradiated with probe sonication at 25 kHz for 1 hour to ensure homogeneous dispersion of FS in the PPy matrix. Finally, the nanocomposite solution was filtered using Whatman filter paper and dried overnight. It was then placed in an oven at 60°C for 9 hours to dry completely. Afterwards, it grounded into powder. The resulting nanocomposites, 1 wt% FS/PPy and 2.5 wt% FS/PPy, are designated as SP1 and SP2, respectively.

To ensure reproducibility, the nanocomposite samples were created under consistent processing conditions, including functionalization time, sonication duration, mixing temperature, and film thickness. Multiple specimens were prepared for each composition to verify consistent electrical and shielding measurements. The film thickness was kept around 1 mm, with minimal variations by maintaining controlled molding conditions.

Potential sources of experimental uncertainty include small variations in thickness, uneven filler dispersion, probe contact resistance, and the sensitivity of the VSWR measurement system. These factors may lead to minor deviations; however, the overall trends and comparative performance between SP1W and SP2W remain dependable and consistent.

Commercially available paraffin wax and SP1 and SP2 nanocomposites were used in this experimental research. A 50 g piece of commercial solid paraffin wax was placed in a 250 ml beaker and melted on a hot plate at 80 °C. To create the composite film (as shown in Figure 2 above), 0.5 g of the prepared nanocomposite particles were separately dispersed into two components, each containing 20 ml of melted paraffin wax. The mixtures were stirred on a magnetic stirrer at a constant temperature of 60 °C for 3 hours to ensure uniform dispersion. Afterward, the mixture was placed in a sonic water bath to ensure proper mixing. To prevent agglomeration, probe sonication was applied at 25 kHz for a total of 20 minutes, using alternating cycles of irradiation and rest at equal intervals. Following sonication, the mixture was poured onto a 1 mm-thick rectangular molding plate and allowed to cool at room temperature until solidified. Once completely solidified, the samples were removed from the mold and prepared for further analysis. The wax-coated samples are designated as SP1W and SP2W, respectively. The prepared composite films were further analyzed through comprehensive analysis. Further, the samples (SP1W & SP2W) were cut into five independent sample with the dimension of 10 mm × 5 mm × 1 mm dimensions for microwave and electrical measurements which were carried out on each specimen to ensure reproducibility.

2.3 Characterization

The crystalline phase of SP1 and SP2 nanocomposites was analyzed using an X-ray diffractometer (X'Pert PRO; PANalytical) with Cu K radiation (1.54056 Å) at a generator voltage of 40 kV and current of 30 mA with a scanning speed of 4º min^{-1} from 10º to 90º. The functional groups of the SP1 and SP2 samples were confirmed by Fourier transform infrared spectroscopy in the wavenumber range from 400 to 4000 cm-1 (FTIR 8400; Shimadzu). The surface morphology was characterized by scanning electron microscopy (SEM, JSM-IT100, JEOL). The VSWR was determined using a microwave test bench (PTPL-8001, Precision Microwave, India) at X-band.

All characterisations were performed under identical experimental condition.

3. Results and Discussion

3.1 Structural analysis

The XRD spectra of the prepared nanocomposite are shown in Figure 3. Generally, a single broad peak around 2θ = 20 to 25° (nearly 22°) confirms the formation of polypyrrole in an amorphous form [18]. With the addition of SWCNT in the case of PPy-SWCNT, the peak appears at 2θ = 26.045° (JCPDS 75–1621) [19] with the 002 plane. The XRD result indicates the peak intensity of the amorphous PPy, indicating the initiation of crystalline nature in the PPy-SWCNT sample.

3.2 Chemical Structure Analysis

In Figure 4, the chemical composition of the prepared PPy/SWCNTs composite has been characterized using FT-IR spectra, typically from 4000 cm-1 to 400 cm-1. An absorption band near 3427 cm−1 is observed in all samples, characteristic of the O–H bond of water, and the band near 1563 cm-1 in pure SWCNT (Figure 4a) corresponds to the carboxylic acid C=O stretching vibration [20]. Characteristic bands of PPy near 658 cm−1 and 932 cm−1 correspond to C–H deformation. Additionally, the peaks near approximately 1,168 cm−1 and 872 cm-1 present the doping state of PPy. The bands centered around 1041 cm−1 and 1179 cm−1 are characteristics of C–H in-plane deformation and N-H stretching vibration, the doping state of PPy, respectively [21]. The results confirm that SWCNTs interact with PPy through π–π stacking without damaging the polymer's backbone structure [22, 23]. FTIR spectra reveal the characteristics of C–H and N–H stretching vibrations, suggesting effective dispersion and intermolecular interactions of SWCNTs within the PPy matrix.

3.3 Morphological Analysis

Figure 5 shows macrophotographic images of the composite films of SP1W and SP2W captured with a digital camera. They are used for further analysis of electrical conductivity and electromagnetic shielding.

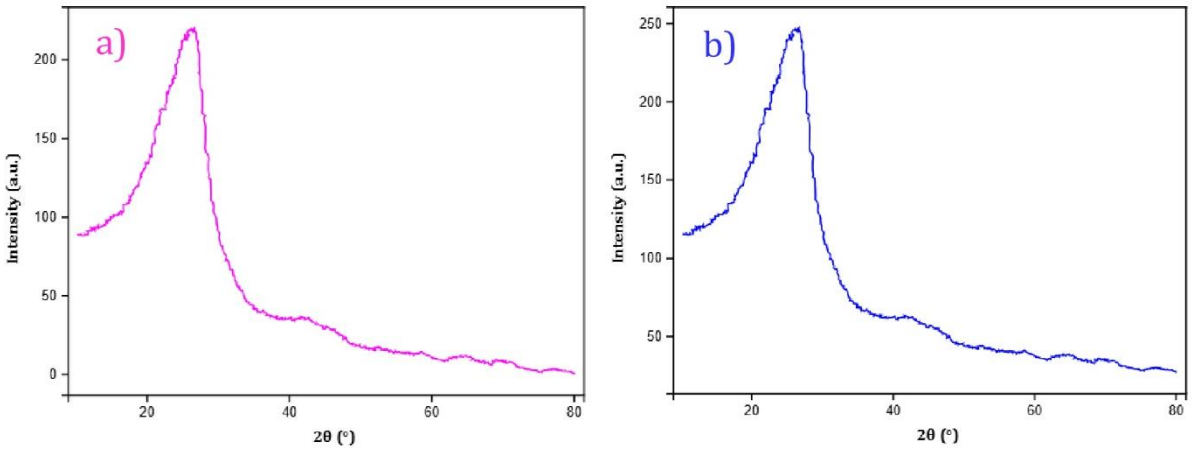

Figure 3. XRD Pattern of **a)** SP1 and **b)** SP2

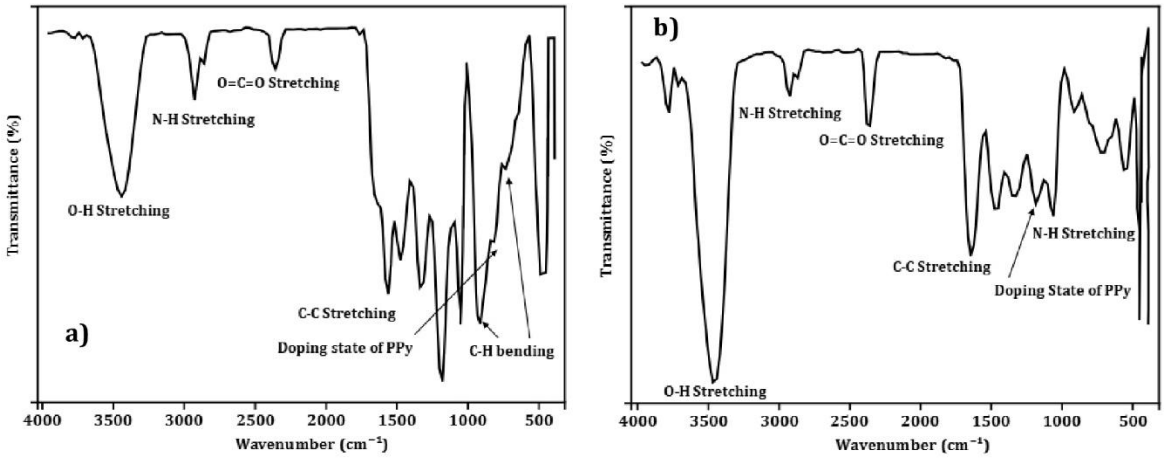

Figure 4. FTIR spectra of **a)** SP1 and **b)** SP2

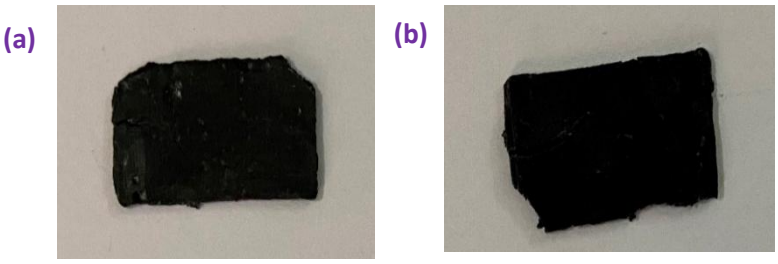

Figure 5. Digital Camera Images of a) SP1W and SP2W

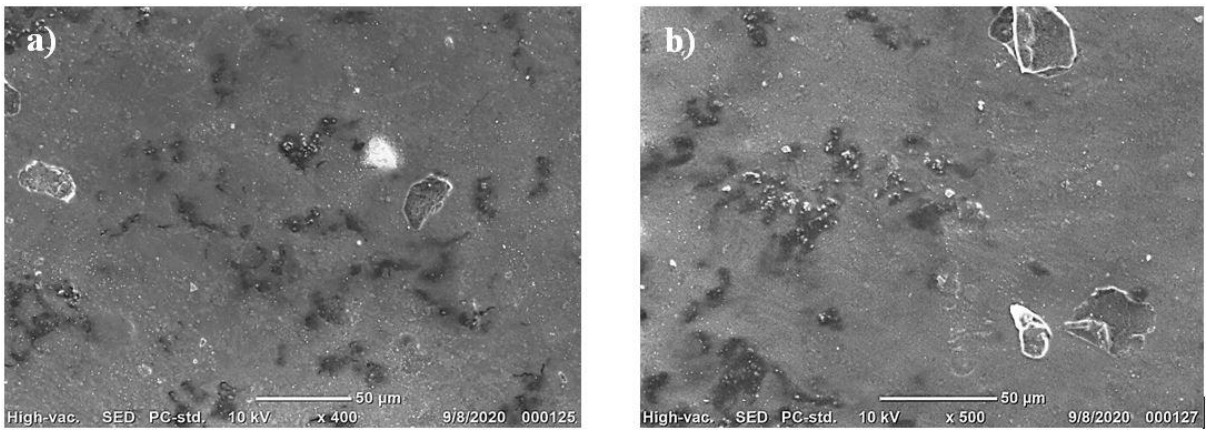

Figure 6. SEM images of **a)** SP1W film and **b)** SP2W film

The surface morphology of the SEM image shows a non-uniform appearance with dark regions, light spots, and irregular patches (see Figure 6). The heterogeneous surface morphology of the SEM has bright regions corresponding to areas of SWCNT fillers, which scatter more secondary electrons. The dark background likely represents SWCNT-rich domains embedded within the PPy-wax matrix. In Figures 6a and b, the SP1W sample exhibits localized agglomerations and microvoids, indicating the filler dispersion and interfacial adhesion of the polymer matrix. This composite seems partially uniform and has well-dispersed fillers. It seems that better dispersion leads to improved electrical conductivity and EMI shielding properties. In contrast, SP2W demonstrates comparatively improved filler distribution and network connectivity. The enhanced dispersion of SWCNTs facilitates the formation of conductive percolation pathways, enabling more efficient electron transport. Improved interfacial interactions between functionalized SWCNTs and PPy reduce contact resistance, contributing to the observed increases in electrical conductivity and shielding effectiveness.

The characterization results (XRD, FTIR, and SEM) confirm the successful formation of PPy/SWCNT nanocomposites. The XRD peak broadening and FTIR signatures indicate effective π–π interactions between PPy and SWCNTs. At the same time, SEM reveals non-uniform dispersion and localized agglomerations in SP1W compared to the more homogeneous distribution in SP2W. These morphological defects directly influence electrical conductivity and shielding effectiveness: poor dispersion leads to higher contact resistance and reduced conductive pathways, whereas improved filler distribution in SP2W facilitates percolation networks, thereby enhancing conductivity and EMI attenuation.

3.4 Electrical Conductivity (σ)

The electrical conductivity of SP1W and SP2W was analyzed using the four-point probe method (Keithley 2400 sourcemeter) to characterize the composite films. SP1W showed evidence of the lowest electrical conductivity of 4.3 S m-1 ± 0.2 S m-1, with a calculated resistivity of 0.233 ± 0.011 Ω·m, and a corresponding sheet resistance for a 1 mm-thick film of 232.6 ± 10.8 Ω/sq. whereas SP2W exhibited the highest value of 11.8 S m^{-1} ± 0.6 S m^{-1}, the calculated resistivity was 0.0847 ± 0.0043 Ω·m, and the corresponding sheet resistance for a 1 mm thick film was 84.8 ± 4.3 Ω/sq. For both samples, the uncertainties were estimated using standard error sheet resistance (ΔRs) and error propagation (Δρ), respectively.

The obtained results showing that the presence of SWCNTs (2.5 wt%) plays a vital role in improving the electrical conductivity of the SP2W due to the strong interconnected conductive network.

3.5 Microwave Shielding Analysis

The Microwave testbench of M/s The Scientific Instrument Co. Ltd. (Figure 7) was used to analyze attenuation measurements using SP1W and SP2W films.

Figure 7. Microwave Test Bench

The procedure followed to measure the attenuation of the samples is as follows:

1. Initially, without connecting the samples to be characterized, the source was energized by applying a beam voltage of 230 V and a repeller voltage of -195 V for the mode maximum condition. Beam current was 18 mA.
2. The Klystron power supply was set to operate in internal modulation mode.
3. The amplitude and frequency of the modulating signal were adjusted to obtain maximum deflection in the Voltage Standing Wave Ratio (VSWR) meter.
4. The VSWR range switch was set at -20 dB. The variable attenuator was adjusted so that the deflection on the VSWR meter read 0 dB (10 log10 P1). It means that the input power at 0 dB is the reference level for measuring the sample's actual attenuation.
5. Now, the samples to be characterized are connected (one at a time) at the appropriate position of "Given attenuator" with the frequency of 9GHz. The dimensions of the attenuator's termination aperture are 1.8 cm x 1 cm.
6. Changed the VSWR range switch appropriately, and the output power was measured in the VSWR panel in dB level.

For sample SP1W, the VSWR panel read 1.34, whereas for sample SP2W, it read 1.27. It indicates that a higher weight percentage of SWCNT in SP2W yielded higher shielding.

For reliable, repeatable measurement with accuracy and reproducibility, the VSWR test was conducted 5 times per sample at 9 GHz under identical operating conditions. The mean value and standard deviation were calculated from these five independent measurements (see Table 1)

Moreover, Return Loss (RL), Mismatch Loss (ML), Reflection Coefficient (RC), skin depth, absorption loss, reflection loss, and multiple reflections are calculated using the following equations to determine shielding effectiveness. [24-27]

The Reflection Coefficient indicates the amount of the incident wave that is reflected.

$$RC = \frac{VSWR-1}{VSWR+1} \quad (1)$$

Return Loss indicates how well a device matches its characteristic impedance.

$$RL\ (dB) = -20log_{10}(RC) \quad (2)$$

VSWR is a measure of the efficient transmission of power from the input to the load.

$$VSWR = \frac{RC+1}{RC-1} \quad (3)$$

Mismatch Loss is actually the power wasted from the incident power due to impedance mismatch.

$$ML\ (dB) = -10log_{10}(1-RC^2) \quad (4)$$

Skin depth of a conductor is defined as the depth into its surface where the amplitude of an electromagnetic wave decreases to 1/e of its value at the surface.

$$Skindepth\ \delta = \sqrt{\frac{2}{\omega\mu 0\sigma}} \quad (5)$$

Here ω=2πf, μ0=4π x 10^{-7} H/m (value in free space)

Absorption loss is the power that is consumed in the medium through which it passes, in the form of heat or other forms of energy.

$$Absorptionloss\ A(dB) = 8.686\frac{t}{\delta} \quad (6)$$

Here t=thickness of the film

Reflection Loss is the power lost due to reflections resulting from impedance mismatch between a transmission line and its load.

$$Reflectionloss\ R(dB) = 20log_{10}\frac{1+RC}{1-RC} \quad (7)$$

The multiple-reflection loss is the power loss due to repeated reflections of the microwave signal caused by impedance mismatch in a transmission line or waveguide.

$$\text{Multiple reflection Loss } B\ (dB) = -20log_{10}\left|1 - |RC|^2 e^{-\frac{2t}{\delta}}\right| \quad (8)$$

$$Total\ SE = A + R + B \quad (9)$$

The shielding mechanisms of reflection loss, absorption loss, multiple reflections, skin depth, reflection coefficient, and conductivity are calculated from the VSWR, as shown in Table 1. As a result, it is attractive to infer the EMI shielding mechanism of materials from reflection and absorption coefficients, which represent the fractions of incident EM waves, rather than from the general terms of Reflection and Absorption.

The EMI shielding behavior of the composites is determined by electrical conductivity, impedance matching, and skin depth–dependent attenuation. The increased conductivity of SP2W reduces the skin depth, enabling greater attenuation of electromagnetic waves within the material due to the strong interconnected network of 2.5 wt% of SWCNT loading on the polymer matrics. As skin depth decreases, electromagnetic energy is dissipated more effectively through absorption mechanisms.

Generlly, Higher conductivity increases the free-charge-carrier density, enhancing reflection at the material surface, while improved conductive pathway promote absorption loss through ohmic dissipation [28]. The combined contributions of reflection, absorption, and multiple internal reflections result in improved total EMI shielding effectiveness for SP2W compared with SP1W (due to the limited conductive network with low loading (~1 wt%)). In particular, the metals and their composites exhibit relatively high shielding performance with reflection-dominant shielding. This characteristic primarily arises from their high electrical conductivity, in which abundant free electrons interact directly with incident EM waves, thereby scattering the radiation power via reflection [29].

However, carbon-based materials such as graphene, CNT, and their composites absorb some EM waves and exhibit absorption-dominant shielding, thereby transforming the EM energy [30]. Note that SP2W gives an SE of ~8 dB more than SP1W, due to the concentration of the 2.5 wt% SWCNT in SP2W, which emphasizes the need for high-performance EM wave-absorbing materials for EM pollution issues.

Table 1. Explaination of the shielding mechanisms

Parameter	SP1W	SP2W	Explanation
VSWR (Voltage Standing Wave Ratio)	1.34 ± 0.02	1.27 ± 0.01	Lower VSWR in SP2W indicates improved impedance matching (Z) and reduced reflection of electromagnetic waves.
Reflection Coefficient (RC)	0.145± 0.003	0.119± 0.002	A decrease in RC with SWCNT loading shows reduced reflected electromagnetic (EM) energy.
Return Loss (RL) (dB)	16.75± 0.15	18.49± 0.18	Higher RL in SP2W indicates better EMI shielding performance and improve attenuation of reflected signals
Mismatch Loss (dB)	0.52 ± 0.01	0.46 ± 0.01	Reduces the signal reflections due to the high loading of SWCNT into the polymer matrics
Electrical Conductivity (σ) (S/m)	4.3± 0.2	11.8± 0.4	Conductivity increases significantly because of better conductive network formed with higher SWCNT.
Skin Depth (δ) (mm)	2.558± 0.05	1.544± 0.04	Reduced skin depth in SP2W suggests stronger EM wave attenuation.
Absorption Loss (A) (dB)	3.395± 0.08	5.624± 0.10	Absorption loss raises with higher SWCNT loading, indicating absorption dominates the shielding behavior.
Reflection Loss (R) (dB)	2.542± 0.05	2.076± 0.04	A slight reduction in reflection loss shows that shielding is more influenced by absorption rather than reflection.
Multiple Reflection Loss (B) (dB)	0.084± 0.01	0.034± 0.01	Internal multiple reflections contribute very littele to overall shielding effectiveness.
Shielding Effectiveness (SE) (dB)	6.02± 0.12	7.73± 0.15	Overall EMI shielding performance improves due to increased conductivity and better absorption mechanisms.

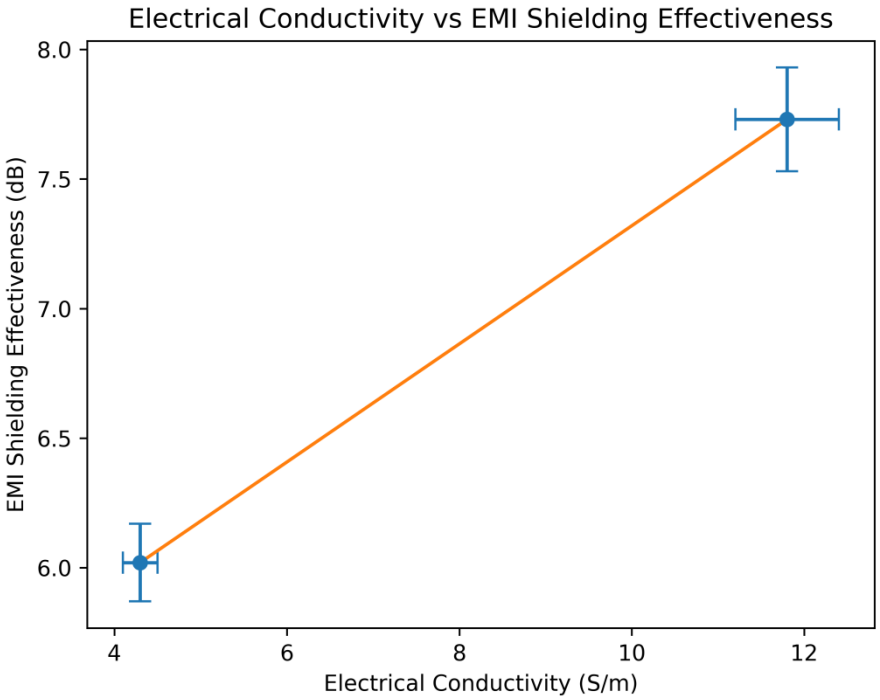

Figure 8. Relationship between Electrical conductivity Vs EMI shielding Effectiveness

Table 2. Comparative studies of SE and Electrical conductivity with the current work

Composite System	CNT Loading	Electrical Conductivity (S/m)	EMI SE (dB)	Remarks	Ref.
PPy/SWCNT–Wax (Current Work)	1 wt%	**4.3 S/m**	6.02	Low CNT loading, lightweight composite	This Work
PPy/SWCNT–Wax (Current Work)	2.5 wt%	**11.8 S/m**	7.73	Improved conductive network formation	
SWCNT/PDMS composite	5 wt%	~85 S/m	–	Higher conductivity due to larger CNT fraction	[31]
CNT/PLA composite	5 wt%	~20 S/m	~67	3D conductive network improves conductivity	[32]
PCL/MWCNT composite	0.25 vol%	~4.8 S/m	60–80	Conductivity comparable to low-loading systems	[33]
Polyamide-6/CNT composite	0.3 wt%	~100 S/m	~25	Conductive percolation network	[34]

As per the observations from the above discussion, the electrical conductivity (4.3–11.8 S m^{-1}) and EMI shielding effectiveness (~6–8 dB) of SP1W and SP2W obtained in this study with 1 wt% and 2.5 wt% SWCNT loaded polymer composites reported in this work (Figure 8). For instance, carbon nanotube/polymer systems with higher filler loading or multilayer architectures have demonstrated shielding values exceeding 20–40 dB due to enhanced conductive network formation and multiple reflection pathways [29, 30]. Similarly, hybrid graphene–CNT–conductive polymer composites have shown superior EMI attenuation owing to synergistic conductive and dielectric losses [12].

However, the present work (Table 2) emphasizes lightweight structure, low SWCNT loading, ease of fabrication, flexibility, and cost-effectiveness. The observation from this present work the increases of conductive fillers (from 1 to 2.5 wt%) approches the electrical percolation threshold which makes efficient charge transport mechanism. Therefore, the results exhibit a direct relationship between SWCNT loading, electrical conductivity, and EMI shielding effectiveness,

where increasing SWCNT concentration improves the formation of conductive network, leading to stronger EM wave absorption and enhanced shielding performance.

4. Conclusion

The study successfully demonstrated the fabrication of PPy/SWCNT nanocomposites wrapped with paraffin wax for EMI shielding applications. The results showed that increasing the SWCNT loading from 1 wt% (SP1W) to 2.5 wt% (SP2W) significantly improved electrical conductivity (from 4.3 S/m to 11.8 S/m) and EMI shielding effectiveness (from 6.02 dB to 7.73 dB), as measured by VSWR. On the whole, SP2W shows better electrical conductivity and EMI shielding performance due to the formation of a more effective conductive network occurs high percolation threshold, while SP1W retains better dispersion with lower filler not near to the percolation threshold with less shielding performance. This enhancement is due to better dispersion of SWCNTs, reduced skin depth, and improved absorption-based shielding mechanisms. The lightweight, cost-effective, and flexible nature of the PPy/SWCNT–wax composites makes them promising candidates for practical EMI shielding in electronic devices that require moderate attenuation. Future studies will focus on optimizing filler loading, exploring hybrid nanofillers, extending the frequency range, and enhancing mechanical and thermal stability to achieve greater shielding effectiveness and industrial scalability.

References

[1] B. Rajesh Kumar, J. Gopu, B. Krithika, V. Akshat, C. Murthy, C.E. Krishna, A Review on Recent Progress in Polymer Composites for Effective Electromagnetic Interference Shielding Properties – Structures, Process, and Sustainability Approaches. Nanoscale Advances, 6, (2024) 5773–5802. https://doi.org/10.1039/D4NA00572D

[2] M.S. Dresselhaus, G. Dresselhaus, A. Jorio, Unusual Properties and Structure of Carbon Nanotubes. Annual Review of Materials Research, 34, (2004) 247–278. https://doi.org/10.1146/annurev.matsci.34.040203.114607

[3] C.W. Nan, Physics of Inhomogeneous Inorganic Materials. Progress in Materials Science, 37, (1993) 1–116. https://doi.org/10.1016/0079-6425(93)90004-5

[4] G. Mittal, V. Dhand, K.Y. Rhee, S.J. Park, W.R. Lee, A Review on Carbon Nanotubes and Graphene as Fillers in Reinforced Polymer Nanocomposites. Journal of Industrial and Engineering Chemistry, 21, (2015) 11–25. https://doi.org/10.1016/j.jiec.2014.03.022

[5] J. Dawei, M. Vignesh, W. Ying, L. Jing, D. Tao, W. Zicheng, S. Qian, W. Chao, L. Hu, L. Na, W. Renbo, S. Angaiah, G. Zhanhu, Electromagnetic Interference Shielding Polymers and Nanocomposites – A Review. Polymer Reviews, 59(2), (2019) 280–337. https://doi.org/10.1080/15583724.2018.1546737

[6] R.P. Avinash, P.A. Nizam, T. Binumol, G. Nandakumar, J. Maciej, P. Claudio, K. Nandakumar, T. Sabu, Recent Progress in Electromagnetic Interference Shielding Performance of Porous Polymer Nanocomposites-A review. Energies, 15(11), (2022) 3901. https://doi.org/10.3390/en15113901

[7] M.N. Norizan, M.R.M. Asyraf, K. Abdan, A. Norli, A.S. Fatimah, H.K. Siti, A. So'bah, M.M. Annie, L. L. Chuan, H.A. Aisyah, N.F.N. Mohd, R.A. Ilyas, M.M. Harussani, M.R. Ishak, S.M. Sapuan, Fabrication, Functionalization, and Application of Carbon Nanotube-Reinforced Polymer Composite: An Overview. Polymers, 13(7), (2021) 1047. https://doi.org/10.3390/polym13071047

[8] Z. Ali, S. Yaqoob, J. Yu, A. D'A, Critical Review on the Characterization, Preparation, and Enhanced Mechanical, Thermal, and Electrical Properties of Carbon Nanotubes and their Hybrid Filler Polymer Composites for Various Applications. Composites Part C: Open Access, 13, (2024) 100434. https://doi.org/10.1016/j.jcomc.2024.100434

[9] D. Feng, D. Xu, Q. Wang, P. Liu, Highly Stretchable Electromagnetic Interference Shielding Segregated Polyurethane/Carbon Nanotube Composites Fabricated by Microwave Selective Sintering. Journal of Materials Chemistry C, 7, (2019) 7938–7946. https://doi.org/10.1039/C9TC02311A

[10] X. Zhang, Y. Li, J. Liu, H. Wang, Ultrathin and Flexible Carbon Nanotube/Polymer Composite Films with Excellent Mechanical Strength and Electromagnetic Interference Shielding. Carbon, 158, (2020) 472–480. https://doi.org/10.1016/j.carbon.2019.11.014

[11] A. Al-Saleh, U. Sundararaj, and Polypropylene/Carbon Nanotube Composite Materials with Enhanced Electromagnetic Interference Shielding Performance: Properties and Modeling. Composites Part B: Engineering, 189, (2020) 107866. https://doi.org/10.1016/j.compositesb.2020.107866

[12] C.L. Lin, J.W. Lin, Y.F. Chen, J.X. Chen, C.C. Chen, C.W. Chen, Graphene nanoplatelet/multiwalled carbon nanotube/polypyrrole hybrid fillers in polyurethane nanohybrids with 3D conductive networks for EMI shielding. ACS Omega, 7(49), (2022) 45697–45707. https://doi.org/10.1021/acsomega.2c06613

[13] Z. Xie, H. Chen, S. Hu, W. Chen, D. Jiang, Graphene/Carbon Nanotube/Polypyrrole Composite Films for Electromagnetic Interference Shielding. Polymer Composites, 44(7), (2023) 3798–3807. https://doi.org/10.1002/pc.27357

[14] X. Lu, Y. Zheng, J. Yang, J. Qu, Multifunctional Paraffin Wax/Carbon Nanotube Sponge Composites with Simultaneous High-Efficient Thermal Management and Electromagnetic Interference Shielding Efficiencies for Electronic Devices. Composites Part B: Engineering, 199, (2020) 108308. https://doi.org/10.1016/j.compositesb.2020.108308

[15] T. Zhang, H. Zou, M. Li, S. Ren, J. Xu, J. Lin, M. Yang, Y. Feng, G. Wang, Polypyrrole Coated Carbon Nanotube Aerogel Composite Phase Change Materials with Enhanced Thermal Conductivity, High Solar-/Electro-Thermal Energy Conversion and Storage. Journal of Colloid and Interface Science, 629, (2023) 632–643. https://doi.org/10.1016/j.jcis.2022.09.103

[16] Y. Cao, Z. Zhao, X. Zeng, High-Performance Polyimide/Polypyrrole-Cnts@PEG Composites for Integrated Thermal Management and Enhanced Electromagnetic Wave Absorption. Advanced Composites and Hybrid Materials, 8, (2025) 104. https://doi.org/10.1007/s42114-024-01202-z

[17] W.L. Song, M.S. Cao, L.Z. Fan, M.M. Lu, Y. Li, C.Y. Wang, H.F. Ju, Highly Ordered Porous Carbon/Wax Composites for Effective Electromagnetic Attenuation and Shielding. Carbon, 77, (2014) 130–142. https://doi.org/10.1016/j.carbon.2014.05.014

[18] U.S. Mohd, H. Ahmad, M. Khan, A. Anees, Synthesis and Characterization of Polypyrrole/Molybdenum Oxide Composite for Ammonia Vapour Sensing at Room Temperature. Polymer Composites, 29, (2021) S989–S999. https://doi.org/10.1177/09673911211036589

[19] B. Ali, S.A. Sami, A. Hasan, N.A. Abdulaziz, M.G. Althobaiti, Cd0.9Co0.1S Nanostructures Concentration Study on the Structural and Optical Properties of Swcnts/PVA Blend. Chemical Physics Letters, 775, (2021) 138701. https://doi.org/10.1016/j.cplett.2021.138701

[20] M. Varga, T. Izak, V. Vretenar, H. Kozak, J. Holovsky, A. Artemenko, M. Hulman, V. Skakalova, D. Su Lee, A. Kromka, Diamond/Carbon Nanotube Composites: Raman, FTIR and XPS Spectroscopic Studies. Carbon, 111, (2017) 54–62. https://doi.org/10.1016/j.carbon.2016.09.064

[21] H. Guo, H. Zhu, H. Lin, J. Zhang, Polypyrrole–Multi-Walled Carbon Nanotube Nanocomposites Synthesized in Oil–Water Microemulsion. Colloid and Polymer Science, 286, (2008) 587–593. https://doi.org/10.1007/s00396-007-1828-0

[22] S. Paul, K.S. Choi, D.J. Lee, P. Sudhagar, Y.S. Kang, Factors Affecting the Performance of Supercapacitors Assembled with Polypyrrole/Multi-Walled Carbon Nanotube Composite Electrodes. Electrochimica Acta, 78, (2012) 649–655. https://doi.org/10.1016/j.electacta.2012.06.088

[23] M.J. Mukulika, P. Chatterjee, D.B. Chakraborty, Charge Transport through Polypyrrole and Single-Walled Carbon Nanotube Composite: A Thermoelectric Material. Journal of Electronic Materials, 51, (2022) 5956–5964. https://doi.org/10.1007/s11664-022-09812-3

[24] L. Pietrzak, S. Ernest, L. Szymanski, The Electromagnetic Shielding Properties of Biodegradable Carbon Nanotube–Polymer Composites. Electronics, 13(11), (2024) 2169. https://doi.org/10.3390/electronics13112169

[25] R. E. Collin, (2001) Foundations for Microwave Engineering. An IEEE Press Classic Reissue.

[26] S.A. Schelkunoff, (1943) Electromagnetic Waves, David Van Nostrand Company, Inc. New York

[27] K.H. Gonschorek, R. Vick, (2010). Skin Effect and Shielding Theory of Schelkunoff. In: Electromagnetic Compatibility for Device Design and System Integration, Springer, Berlin, Heidelberg. https://doi.org/10.1007/978-3-642-03290-5_17

[28] M. Moniruzzaman, K.I. Winey, Polymer Nanocomposites Containing Carbon Nanotubes. Macromolecules, 39(16), (2006) 5194–5205. https://doi.org/10.1021/ma060733p

[29] N.C. Das, Y. Liu, K. Yang, W. Peng, S. Maiti, H. Wang, Single-walled Carbon Nanotube/Poly (Methyl Methacrylate) Composites for Electromagnetic Interference Shielding. Polymer Engineering & Science, 49, (2009) 1627–1634. https://doi.org/10.1002/pen.21384

[30] M.H. Al-Saleh, W.H. Saadeh, U. Sundararaj, EMI Shielding Effectiveness of Carbon-Based Nanostructured Polymeric Materials: A Comparative Study. Carbon, 60, (2013) 146–156. https://doi.org/10.1016/j.carbon.2013.04.008

[31] O. Hur, B.H. Kang, S.H. Park, Optimization of Electrical and Mechanical Properties of A Single-Walled Carbon Nanotube Composite Using a Three-Roll Milling Method. Materials Chemistry and Physics, 309, (2023) 128354. http://doi.org/10.1016/j.matchemphys.2023.128354

[32] O. Lekshmi, C. Anoop, E.J. Reenu, W. Runcy, C.G. Kalapurackal, V.U. Nellipparambil, S.V. Steffy, G. Gejo, M.S. Sanu, P. Issac, Recent Advances in Polymer Nanocomposites for Electromagnetic Interference Shielding: A

Review. ACS Omega, 7(30), (2022) 25921–25947. https://doi.org/10.1021/acsomega.2c02504

[33] J.M. Thomassin, C. Pagnoulle, L. Bednarz, I. Huynen, R. Jerome, C. Detrembleur, Foams of Polycaprolactone/MWNT Nanocomposites for Efficient EMI Reduction. Journal of Materials Chemistry, 18(7), (2008) 792–796. https://doi.org/10.1039/b709864b

[34] A.H.A. Hoseini, M. Arjmand, U. Sundararaj, M. Trifkovic, Significance of Interfacial Interaction and Agglomerates on Electrical Properties of Polymer-Carbon Nanotube Nanocomposites. Materials & Design, 125, (2017) 126–134. https://doi.org/10.1016/j.matdes.2017.04.004

Acknowledgement

The authors thank the management of Geethanjali College of Engineering and Technology & KLEF Deemed to be University for their support.

Authors Contribution Statement

O.V.P.R. Sivakumar: Methodology, Investigation, Writing - Original Draft. Arunmetha Sundaramoorthy: Conceptualization, Investigation, Writing - Review & Editing, Supervision. Dhineshbabu Nattanmai Raman: Validation, Formal analysis, Investigation, Writing - Review & Editing. A. Geetha Rani: Investigation, Data Curation. All the authors have read and agreed to the published version of the manuscript.

Funding

The work was supported by the Department of Science and Technology, India, through the PURSE scheme (SR/PURSE/ 2023/196).

Competing Interests

The authors declare that there are no conflicts of interest regarding the publication of this manuscript.

Data Availability

The data supporting the findings of this study can be obtained from the corresponding author upon reasonable request.

Has this article screened for similarity?

Yes